Bias-free electro-optic polymer-based two-section Y-branch waveguide modulator with 22 dB linearity enhancement

Beomsuk Lee,[1,*] Cheyun Lin,[1] Xiaolong Wang,[2] Ray T. Chen,[1] Jingdong Luo,[3] and Alex K. Y. Jen[3]

[1]*Microelectronics Research Center, The University of Texas at Austin, 10100 Burnet Road, Austin, Texas, 78758, USA*
[2]*Omega Optics, Inc., 10435 Burnet Road, Suite 108, Austin, Texas, 78758, USA*
[3]*Department of Material Science and Engineering, University of Washington, Seattle, Washington, 98195, USA*
**Corresponding author: bslee74@gmail.com*

Received July 1, 2009; revised August 17, 2009; accepted August 24, 2009;
posted September 30, 2009 (Doc. ID 113596); published October 22, 2009

A bias-free two-section Y-branch directional coupler modulator with high linearity based on domain-inverted modulation is fabricated and tested. 25 wt. % AJLS102/APC is used as an active core layer with an experimentally confirmed device r_{33} value of 56 pm/V at 1.59 μm. The fabricated device shows an extinction voltage of 4 V. A two-tone test is performed to demonstrate 64 dB distortion suppression at 25% modulation depth, which is 22 dB higher than a conventional Mach–Zehnder modulator. © 2009 Optical Society of America

OCIS codes: 250.2080, 250.4110, 250.5460.

A Mach–Zehnder modulator (MZM) made of lithium niobate ($LiNbO_3$) is the most common type of commercially available electro-optic (EO) modulator, but its performance has several intrinsic limits. First, the operating point of an MZM needs to be biased to maintain a higher switching depth with better linearity [1]. Second, the transfer curve of an MZM is sine square, which intrinsically contains nonlinear Fourier components that degrade device performance for rf photonics and sensor applications where a linearized transfer curve is highly desired. To address these issues, various linearization techniques have been proposed and studied. These include dual polarization [2], dual parallel modulation [3], cascaded MZM [4,5], and ring-resonator assisted MZM [6]. However, these linearization techniques all come at a cost of increased device complexity. High linearity can also be achieved by carefully designing a Y-branch directional coupler modulator (YDCM) with inverted domains. The theoretical basis for the domain-inverted YDCM was established by Kogelnik *et al.* [7]. Tavlykaev *et al.* theoretically investigated how the linearity of a YDCM can be improved by carefully designing inverted domains [8], and this was experimentally confirmed by [9]. Owing to its symmetric structure, YDCM is intrinsically set at half-power point, eliminating a dc bias requirement. Linearization techniques for YDCM, such as domain inversion and photobleaching, have been investigated by several groups [10,11]. In this Letter, we design and experimentally demonstrate a linearized YDCM based on two-section domain-inverted modulation. The fabricated device shows a highly linear transfer curve. A standard two-tone test is performed to demonstrate the third-order intermodulation distortion (IMD3) suppression of 64 dB at 25% modulation, which is 22 dB higher than a conventional MZM.

The refractive index of an EO polymer is a function of an applied electric field. When an external electric field is applied to one arm of the directional coupler, the refractive index will change in response to the applied electric field and induce a mismatch in the propagation constant ($\Delta\beta$) between the two arms. In a two-section directional coupler with inverted domains, it can be shown that the sign of $\Delta\beta$ would be opposite in the neighboring section owing to the opposite polarity of applied voltage. This $\Delta\beta$ inversion can induce the suppression of IMD3, which is an important criterion representing the nonlinearity of device performance [8,10]. Note that the highly linear performance is derived from the device structure itself instead of from complex external linearization techniques [2–5]. The electrode geometry of the two-section YDCM shown in Fig. 1 is designed such that the polarity of the applied voltage is opposite in the adjacent section. This electrode design simplifies the poling process while achieving the same effect as inverted domains. A lumped electrode design is, however, valid only for low-frequency characterization, typically in kilohertz range, and needs to be replaced by a traveling-wave electrode design for high-frequency characterization in the future.

Figure 2 is our simulation result showing the relative level of distortion suppression in a two-section YDCM at a modulation depth of 1%. Distortion suppression, which is defined as the ratio of fundamental signal (P_{fund}) to distorted signal (P_{dist}), is calculated

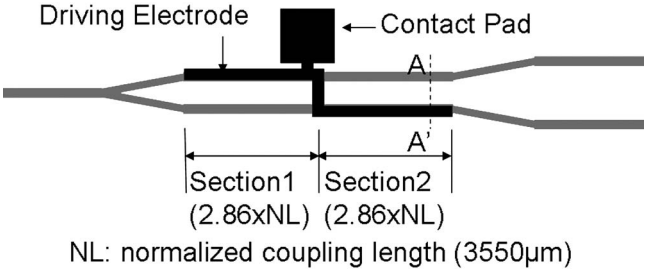

Fig. 1. Schematic illustration of a lumped driving electrode design for two-section YDCM.

0146-9592/09/213277-3/$15.00

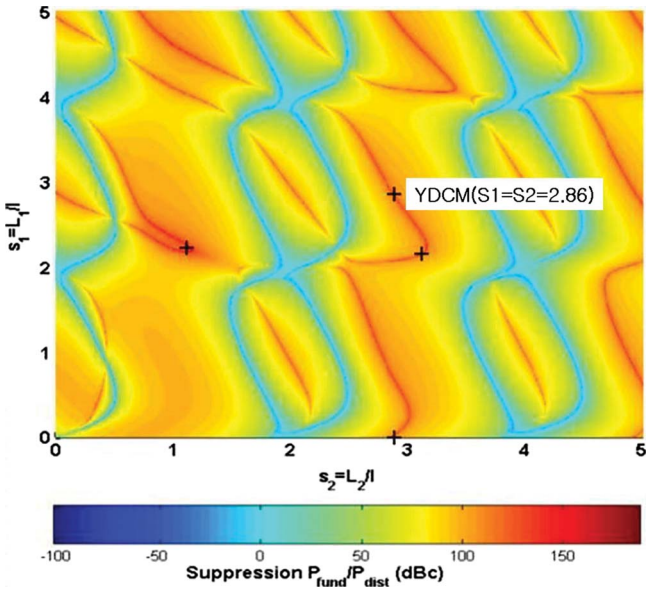

Fig. 2. (Color online) Relative level of distortion suppression in two-section YDCM.

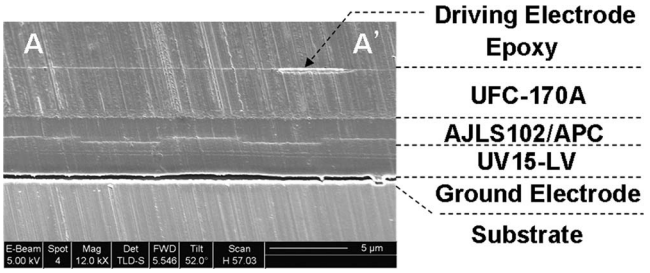

Fig. 3. Cross-sectional scanning electron micrograph of the fabricated device (A-A' corresponds to the reference line in Fig. 1).

as a function of the normalized length of each section (s_1 and s_2). $L1$ and $L2$ are the length of each section, and l is the coupling length of directional coupler. A two-tone numerical procedure is used to calculate the level of distortions [8]. The level of IMD3 is calculated by applying Fourier analysis to the time-dependent optical outputs coming from a two-section YDCM with two electrical input signals of slightly different frequencies applied to the electrodes. The point at $s_1=s_2=2.86$ is chosen for further evaluation in this work.

The device is fabricated by standard semiconductor processes such as spin coating, photolithography, oxygen plasma reactive ion etching (RIE), and wet etching. The active core layer is 25 wt. % AJLS102/APC (amorphous polycarbonate), and the lower and upper cladding layers are UV15-LV and UFC-170A, respectively. The inverted rib waveguides are patterned on UV15-LV layer by photolighography and oxygen plasma RIE. This polymer waveguide structure is sandwiched between the aluminum bottom electrode and the gold top electrode. A contact poling technique is used to pole AJLS102/APC with a poling field of 100 V/μm. With the poling voltage applied at room temperature, the device is heated up to 135°C at the ramping speed of 10°C/min and then cooled down to room temperature. After poling, the gold top electrode layer is patterned into the driving electrodes by photolithography and wet etching. In the last step, the fabricated device is cleaved and polished at both ends for testing. Figure 3 is a cross-sectional scanning electron micrograph of the fabricated device, and A-A' is the reference line representing the device area corresponding to Fig. 1. The waveguide width is 5 μm, and the center-to-center separation between waveguides is 10 μm. The thicknesses of UV15-LV, AJLS102/APC, and UFC-170A are 3.5, 1.5, and 3 μm, respectively. The step height of the rib waveguide is 0.4 μm. The measured in-device r_{33} value is 56 pm/V using the reference MZM fabricated on the same wafer with the two-section YDCM.

The two-section YDCM is tested at $\lambda=1.59$ μm, at which the waveguide supports a TM single mode. The device is tested at the coupling stage of a four-axis Newport auto aligner for precise alignment and light coupling. A TM-polarized laser is launched and coupled into the device with a polarization-maintaining fiber. The output light is coupled into a single-mode fiber that is connected to a photodetector. The total optical loss is measured to be −27 dB, which is very high considering the material propagation loss of −6 dB (−2 dB/cm of AJLS102/ACP times the total device length of 3 cm) and typical coupling loss of −10 dB. This high loss is attributed to the roughness of the input and output facets and possibly the waveguide walls after the RIE process. Figure 4 shows the measured output optical signals of the

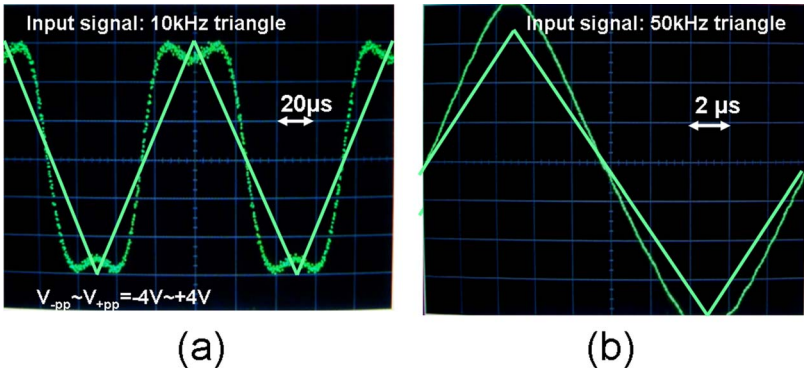

Fig. 4. (Color online) (a) Over-modulation of two-section YDCM at $\lambda=1.59$ μm by an rf signal of 10 kHz with −4V−+4 V, (b) transfer curve of two-section YDCM at $\lambda=1.59$ μm modulated by rf signal of 50 kHz.

two-section YDCM as a function of the applied voltage. Figure 4(a) represents the overmodulation at 1.59 μm. The extinction voltage is measured to be 4 V, which is much reduced from our previous work [10] owing to improvements in EO polymer properties and fabrication techniques. Figure 4(b) shows a highly linear transfer curve at 1.59 μm.

A standard two-tone test is performed to test the distortion suppression ratio of the fabricated device. The testing setup is shown schematically in Fig. 5(a). Two driving signals of 50 and 55 kHz are combined and applied to the device. A modulated output optical signal is coupled into a single-mode fiber that is connected to a photodetector with a built-in amplifier (Throlabs, PDA-400). The converted electrical signal is analyzed by an HP8563E microwave spectrum analyzer. Figure 5(b) shows the rf response of the tested two-section YDCM. The applied rf power is $-0.5\text{V}-+0.5$ V, which is equivalent to 25% modulation depth of the tested device. Fundamental signals at f_1 (50 kHz) and f_2 (55 kHz) are measured to be -27.8 dBm, and the resulting IMD3s at $2\times f_1$-f_2 (45 kHz) and $2\times f_2$-f_1 (60 kHz) are experimentally confirmed to be -92.13 dBm. The achieved distortion suppression is 64 dB. It is necessary to characterize the distortion introduced by the testing setup in order to confirm that 64 dB suppression is derived purely from the device itself. Generally, the biggest source of nonlinear distortion in a testing setup is the amplifier that is used to amplify the electrical signal converted from the detected optical signal. Considering the transimpedance gain (1.5×10^5 V/A) and the responsivity ($\sim$0.9 A/W) of PDA-400, the voltage converted from the modulated optical signal is calculated to be $\sim$6.7 V, which is low enough compared with the saturation limit (10 V) to exclude possible extra nonlinear distortion from the amplifier. Our theoretical calculation expects that the distortion suppression of 58 dB can be achieved at 25% modulation depth. Extra 6 dB suppression can be attributed to experimental errors, i.e., the fluctuation of the output signal and possibly undermodulation due to external perturbation. Theoretical calculation shows that conventional MZM has a distortion suppression of 42 dB at 25% modulation depth. Our device shows 22 dB improvement over conventional Mach–Zehnder structure.

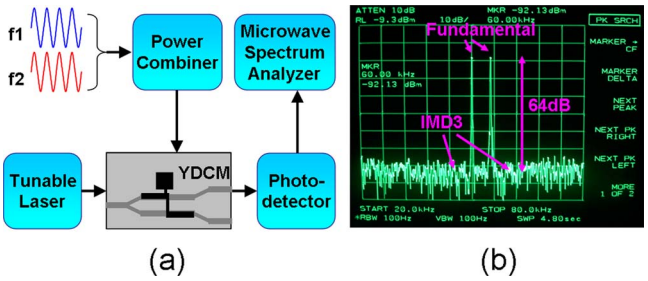

Fig. 5. (Color online) (a) Block diagram of the testing setup, (b) rf response of two-section YDCM tested at $\lambda = 1.59$ μm.

In conclusion, a bias-free YDCM based on the domain-inverted modulation of an EO polymer is fabricated and tested at 1.59 μm. A two-tone test of the fabricated device is demonstrated with an IMD3 suppression of 64 dB at 25% modulation depth, which is 22 dB higher than conventional Mach–Zehnder structure.

The authors thank the gracious support of the Defense Advanced Research Projects Agency (DARPA) (W31P4Q-08-C-0160) on this research.

References

1. D. An, Z. Shi, L. Sun, J. M. Taboada, Q. Zhou, X. Lu, R. T. Chen, S. Tang, H. Zhang, and W. H. Steier, Appl. Phys. Lett. **76**, 1972 (2000).
2. L. M. Johnson and H. V. Roussell, Opt. Lett. **13**, 928 (1988).
3. S. Korotky and R. de Ridder, IEEE J. Sel. Top. Quantum Electron. **8**, 1377 (1990).
4. H. Skeie and R. V. Johnson, Proc. SPIE, **1583**, 153 (1991).
5. D. Raskin, K. Chiang, and J. Stamatoff, "Cable system incorporating highly linear optical modulator," U.S. patent 5,031,235 (July 9, 1991).
6. A. Prescod, B. B. Dingel, and N. Madamopoulos, *Broadband Access Communication Technologies III*, A. Prescod, B. B. Dingel, and N. Madamopoulos, eds. (SPIE, 2009), Vol. 7234, p. 72340E.
7. H. Kogelnik and R. Schmidt, IEEE J. Quantum Electron. **12**, 396 (1976).
8. R. Tavlykaev and R. V. Ramaswamy, J. Lightwave Technol. **17**, 282 (1999).
9. T. Kishino, R. F. Tavlykaev, and R. V. Ramaswamy, IEEE Photon. Technol. Lett. **12**, 1474 (2000).
10. S. Tang, Z. Shi, D. An, L. Sun, and R. T. Chen, Opt. Eng. **39**, 680 (2000).
11. Y. C. Hung, S. K. Kim, H. Fetterman, J. Luo, and A. K. Y. Jen, IEEE Photon. Technol. Lett. **19**, 1762 (2007).